Contact mechanics of isotactic polypropylene

Contact mechanics of isotactic polypropylene: Effect of pre-stretch on the frictional response

Stan F.S.P. Looijmans, Patrick D. Anderson, Lambèrt C.A. van Breemen*

Polymer Technology, Department of Mechanical Engineering, Eindhoven University of Technology, P.O. Box 513, 5600 MB Eindhoven, The Netherlands

Abstract

Polymers are increasingly used in applications where relative moving parts are in contact. The dissipation of energy due to friction, i.e. heat production, reduces a product's lifetime significantly. Since in processing often an extrusion or injection moulding step is used in product formation, the induced anisotropic microstructure leads to a spatial variation of mechanical properties, for example frictional resistance. In this work we compare the scratch response of isotropic isotactic polypropylene (iPP) to the response of various oriented iPP systems. Subjected to single-asperity contact with a rigid diamond, the surface penetration and lateral force are measured. For various combinations of applied normal load and sliding velocity, the surface penetration and lateral force are measured. Optical profilometry measurements are used to explain the (large) differences in residual scratch profile between tests performed in the direction parallel and transverse to the orientation direction, respectively. As the anisotropy increases with the amount of orientation, both the maximum tensile stress and the strain hardening increase substantially. The penetration depth, for oriented systems governed by the transverse viscoelasticity and yield stress, is comparable for all loading angles and decreases with increasing amount of orientation. The direction of lowest frictional resistance is shown to be the direction parallel to the oriented crystals. The combination of decreasing global deformation and friction reduction as a result of pre-stretch decelerates strain localization, therewith delaying crack initiation which eventually leads to abrasive wear. Along with that, the substantial amount of elastic recovery after scratching in the transverse direction is related to the pre-tension of the perpendicular crystal network.

Keywords: Sliding friction, Contact mechanics, Scratch testing, Polymers

1. Introduction

The advanced physical properties that polymers can display, e.g. light-weight, self-lubricating or corrosion resistant, make them an interesting alternative for metal parts in many structural and dynamic applications. Particularly semi-crystalline materials, i.e. materials that partially crystallize upon solidification, are widely used in automotive industry and in medical implants [1–6]. In these products, surface contact is a challenging subject because of complex loading conditions involving many variables [7–10]. Simplification to a well-defined contact situation is required for proper analysis; in this work we consider a single-asperity sliding friction experiment, often referred to as "scratch-test". This test allows to study a wide range of loading conditions in a controlled manner [11, 12].

Friction is generally understood as being the resistance encountered by one body sliding over another. Since little is known about local contact phenomena causing frictional resistance, extensive long-term testing is often required and life-time predictions mostly turn out wrong. Reason for this, is the determination of the true, in-situ, contact area in a sliding friction experiment, which is usually approximated being either ideal elastic, ideal plastic, or combinations thereof [7, 12–14]. However, due to the non-linear viscoelastic nature of polymers this is a strong assumption; the complex interplay between compressive and tensile stresses leads to development of a so called "bow-wave", significantly changing the real area of contact. More accurate is the estimate of this area from the residual deformation [15] or in the case of transparent materials, the in-situ observation, using a microscope mounted at the back-surface of the sample [16, 17].

To circumvent these challenges, over the last two decades Finite Element Methods (FEM) computations are increasingly employed to study non-linear contact problems in a qualitative [18–25], and quantitave way [26, 27]. Numerical scratch simulations, validated by experiments, are a powerful tool in the visualization of the complex deformation field, i.e. stress and strain distribution. In the recent past, hybrid experimental/numerical studies have been performed on the contact mechanics of glassy polymers. Starting with polycarbonate (PC) as a well-characterized

*Corresponding author

Email address: L.C.A.v.Breemen@tue.nl (Lambèrt C.A. van Breemen)

model-system, the experimentally observed scratch response was accurately simulated by Van Breemen, using solely the intrinsic material behaviour [26]. To describe the deformation kinetics, constitutive modelling is done using the Eindhoven Glassy Polymer model (EGP-model) [28–32]. In the recent past, this methodology is used by Krop (2016) to quantitatively describe the intrinsic material response of particle-filled glassy [27, 33] and thermoset composites [34], and successively predict their scratch response up to the point where brittle machining sets in.

In practice however, the use of semi-crystalline materials is desired due to their low-cost and processability. Their physical and mechanical properties strongly depend on the crystal structure and super-molecular morphology induced during processing of the material. This includes both the chemical and thermo-mechanical history; polymerization where chemical composition, chain architecture and molecular weight can be altered and product design where material formulation, pressure, flow and cooling rates determine the final mechanical properties [35, 36]. Since commonly an extrusion or injection moulding step is involved in the production process, large spatial variations of cooling rate, pressure and flow lead to anisotropy and local chain orientation [35–37].

In this work we study the surface mechanics of the widely used semi-crystalline polymer isotactic polypropylene (iPP). The recent characterization of the intrinsic material properties of its individual polymorphs [38] and its high drawability [37], make it well-suitable for the study of anisotropy in the form of crystal orientation. For various amounts of pre-orientation, the in-situ scratch response as well as the residual scratch profile is compared to those of isotropic samples. Uniaxial, solid-state drawing significantly increases the scratch resistance of iPP in both principal directions, i.e. parallel and perpendicular to the drawing direction.

2. Materials and methods

Materials

An iPP homopolymer provided by SABIC (Riyad, Saudi Arabia) is used to prepare isotropic samples; an injection moulding grade with a weight average molecular weight $M_w = 320$ kg/mol and polydispersity $M_w/M_n = 5.4$. This grade was selected because its yield kinetics are recently determined by Caelers et al. [38]. The material is synthesized with Ziegler-Natta catalyst and has a high tacticity. A highly stereo-regular homopolymer, provided by Borealis (Vienna, Austria) with weight average molecular weight $M_w = 365$ kg/mol, polydispersity $M_w/M_n = 5.4$ and tacticity 97.5% [mmmm] is used to prepare oriented tapes. This particular grade is selected because it has already been used in several crystallization studies [35, 36]. Moreover its melt flow index is equal to 8.0 (230 °C/2.16 kg), making it a suitable material for film extrusion.

Sample preparation and characterization

Indentation and single-asperity sliding friction tests are performed on the micro-scale. Given the dimensions of the indenter tip, the surface roughness is limited to 100 nm in order to make a proper distinction between the surface roughness and the actual tribological experiment. Hence, to prepare isotropic samples, polymer granules are molten using a hot stage at a temperature of 230 °C, manually compressed between two microscope glass slides to a thickness of about 500 µm, and kept isothermal for 10 min to erase any thermo-mechanical history. Subsequently the material is quenched to room temperature between thick aluminum plates. In the following this sample is addressed as ISO.

Continuous films are mono-extruded using a single-screw extruder (Davis-Standard Limited, CT, USA), fitted with an 100 mm die. The temperature profile from feed-in zone to die is gradually increased from 180 °C to 230 °C. A gear pump is placed between extruder and die to ensure a steady feed flow of 1 m/min. Collin CR 136/350 chill rolls are used to quench the extrudate to 15 °C under a pressure of 50 bar, and subsequently collect the solidified film with a thickness of 400 µm on a spool.

Orienting the extruded samples is done off-line in cooperation with DSM (Geleen, the Netherlands) by means of two techniques; a confined calendar set-up is used to reduce the thickness of the sample by a factor 2, while preserving the width of the sample. After calendering the sample at 120 °C the samples are quenched to room temperature to preserve the induced orientation. Draw ratios up to DR = 5 are achieved by solid state drawing over a short gap at 120 °C and subsequent quenching to room temperature. The draw ratio is defined as the speed ratio of the inlet compared to the outlet goddet. In the following the slightly anisotropic extruded, calendered and drawn samples are addressed as DR-1.1, DR-2 and DR-5, respectively. From the resulting films dogbone shaped samples of 12 mm x 5 mm are cut in the two principal directions to be used for tensile testing. Samples of approximately 20 mm x 20 mm are cut manually from the center of the film and subsequently used for the sliding friction experiments.

To determine the surface roughness of the samples and to characterize the residual profile of the scratch after the sliding friction experiment, a Sensofar Plµ 2300 optical profilometer is used. After a sample is horizontally aligned the system is moved along the z-axis (normal to the sample's surface) over a distance of 20-40 µm, depending on the sample and the scratch depth. Three-dimensional profiles are acquired using a Nikon Plan Fluor 50x/0.80 EPI lens, leading to a resolution of 0.2 µm in Z-direction. In-plane resolution is given by the pixel size of the detector, which is 0.332 µm for this set-up. The surface roughness of all samples considered in this work is checked and found to be well below 1% of the in-situ surface penetration, and therefore not influences the scratch test.

The anisotropy of the solid state drawn tapes is characterized using synchrotron X-ray diffraction at the Euro-

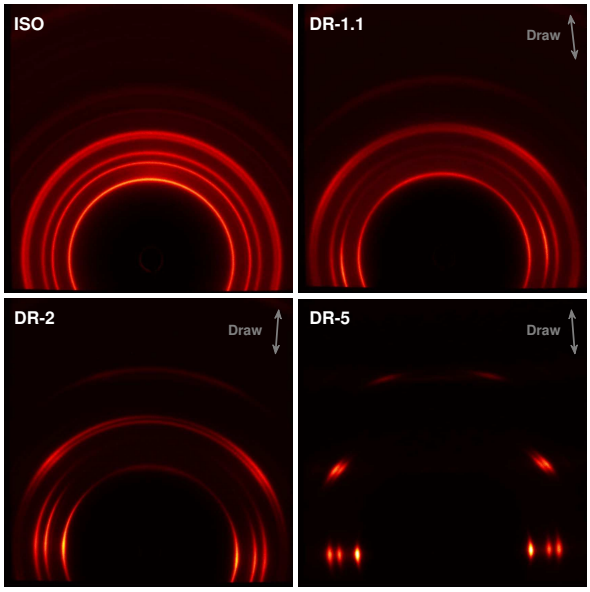

Figure 1: Normalized, background subtracted WAXD patterns for isotropic and oriented iPP samples. All samples are composed of solely α-iPP crystals and amorphous phase. Upon increasing pre-stretch the diffracted photons concentrate to specific angles for each crystal plane. The drawing direction is indicated by the gray arrow in each frame.

pean Synchrotron Radiation Facility (ESRF) in Grenoble, France. The Dutch-Belgian Beamline 26B (DUBBLE) [39] with a wavelength of $\lambda = 1.033$ Å and frame time of 60 sec is used to record two-dimensional Wide-Angle X-ray Diffraction (WAXD) patterns, using a Frelon2K dark current detector with a pixel size of 48.8 µm x 48.8 µm. The software FIT2D is used to visualize and integrate the data. All presented statistics are background subtracted and normalized for the instant beam intensity.

Wide-angle diffraction patterns of the solid-state drawn samples, presented in Figure 1, show besides the orientation, a pattern not dissimilar from the one obtained for isotropic α-phase iPP (top-left frame), indicating that the tapes as prepared by extrusion consist of solely iPP α-phase [40, 41]. Upon increasing the amount of orientation, a concentration towards the equator can be seen for the (110), (040) and (130)-planes and to 39° and 38° for the (111) and (041)-planes respectively.

Mechanical testing

Dogbone shaped samples of 12 mm x 5 mm are cut from the extruded and subsequently stretched tapes. Uniaxial tensile experiments are performed on a Zwick Z5.0 universal tensile tester, equipped with a 5 kN load cell. A constant engineering stretch-rate in the range of $\dot{\epsilon}_e = 10^{-5}$ to 10^{-1} s^{-1} is applied to determine the tensile yield stress at ambient temperature (23 °C); for the samples labelled DR-1.1 and DR-2 in both the machine direction (MD) as well as the transverse direction (TD), and for DR-5 (due to homogeneous sample dimensions) only in machine direction. A pre-load of 0.1 MPa is applied at a speed of 1 mm/min to ensure a positive tensile stress at the beginning of the experiment. Tests are performed at least in duplicate, to ensure reproducibility.

Single-asperity sliding friction experiments are performed using an MTS Nano Indenter XP; by the application of a defined normal load and sliding velocity measuring the surface penetration and lateral force. A diamond indenter tip geometry, conical shaped with a cone angle of 90 ° and a top radius of 50 µm is used to apply normal loads in the range of 200-500 mN. Two rotational motors control the linear, in-plane motion and are, after an indentation step, capable of applying sliding velocities over four decades of magnitude in both the machine direction as well as the transverse direction. Scratch tests with a length of 1 mm are performed at scratch velocities ranging from 0.1 to 100 µm/s, all at room temperature. Each combination of sliding velocity and normal force is applied at least three times to check reproducibility of the steady-state penetration depth and friction force.

3. Results and discussion

Isotropic polypropylene

Compared to a uniaxial compression test, where there is homogeneous deformation and a constant strain-rate, or a simple uniaxial tensile test, in a single-asperity sliding friction experiment the deformation of the material is relatively complex. When scratching the indenter tip over a polymer surface, the zone beneath the tip and in front of the tip is compressed, whereas behind the tip the material experiences a tensile stress. In the contact zone between diamond and polymer large shear stresses are present. To compare materials with various mechanical properties, understanding the influence of the applied test parameters on the reference sample is essential. In a scratch experiment, the control parameters are the applied normal force and the sliding velocity. In-situ, the momentary penetration into the surface and friction (lateral) force are measured as a function of the position along the scratch direction. Since the experiment is force controlled, after a scratch velocity independent indentation step, at the onset of lateral movement the loss of contact area between indenter and surface causes the tip to sink into the material. Thereafter, a bow-wave develops and stabilizes the area of contact over time. Steady-state values for the surface penetration and lateral force are presented in Figure 2 for various applied loads and sliding velocities.

The penetration depth decreases with increasing sliding velocity (Figure 2a). For polymers, and more general for viscoelastic materials, it is known that the yield point, i.e. the stress-level at which the plastic flow rate equals the applied deformation rate, increases with increasing deformation rate. By applying a higher global scratch velocity, local deformation rates increase, and therewith also the resistance against deformation. As a result, the steady-state regime of the friction force is closely related to the penetration depth; a lower surface penetration means less material

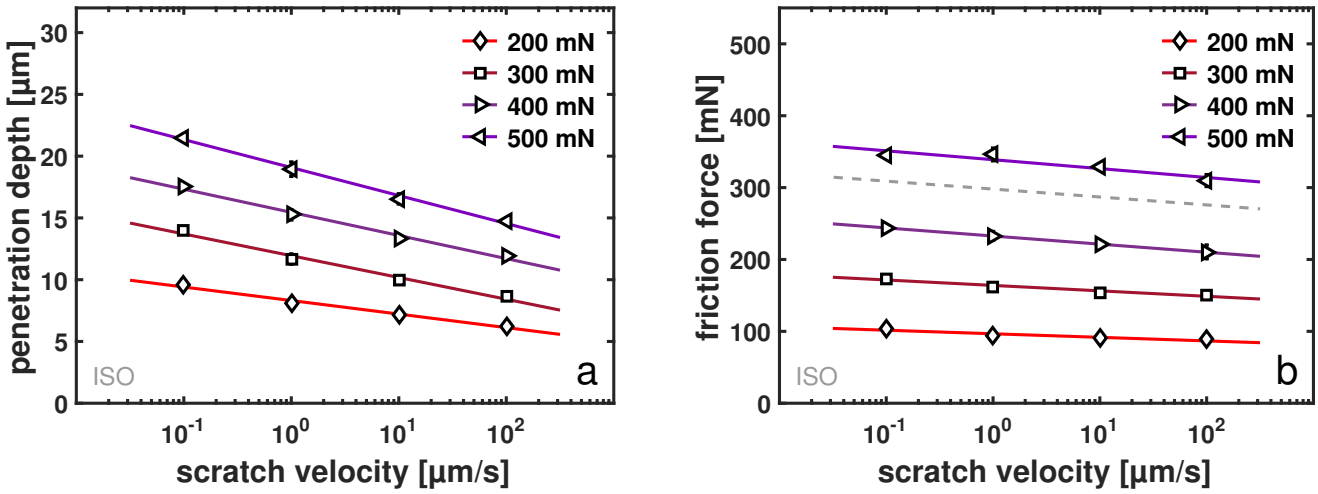

Figure 2: a) Penetration depth as function of the applied sliding velocity for different normal loads measured on isotropic samples. b) Lateral friction force as function of the applied sliding velocity. Crack formation at an applied load exceeding 500 mN leads to an extra increase in lateral force. Expectation for the friction force for ductile deformation is indicated with the dashed line.

to be displaced, hence a lower frictional force (Figure 2b). Both measured variables are linear when plotted against the logarithm of scratch velocity.

The second important parameter, the normal load that is applied on the sample, is varied between 200 and 500 mN. With increasing load, the penetration into the surface increases (Figure 2a), and with that the friction force increases (Figure 2b). Since the indenter tip has a conical shape, a larger penetration depth results in a larger plastic zone around the indenter tip, due to a higher applied load. When a larger fraction of the total deformation is of viscoplastic nature, the velocity dependence of the penetration depth increases. The velocity dependence of the friction force however, is affected by the increasing velocity dependence of the penetration depth. Recalling that the friction force is determined by the bow wave in front of the tip, the intrinsic large-strain kinetics explain this; the material that accumulates in front of the indenter tip and forms the bow wave, was originally situated in a location near or below the tip. The large deformations in that area lead to local strain hardening effects, which in general can be considered to have a non-constant strain-rate dependency. For isotactic polypropylene however, the viscous contribution in strain hardening is negligible (as can be

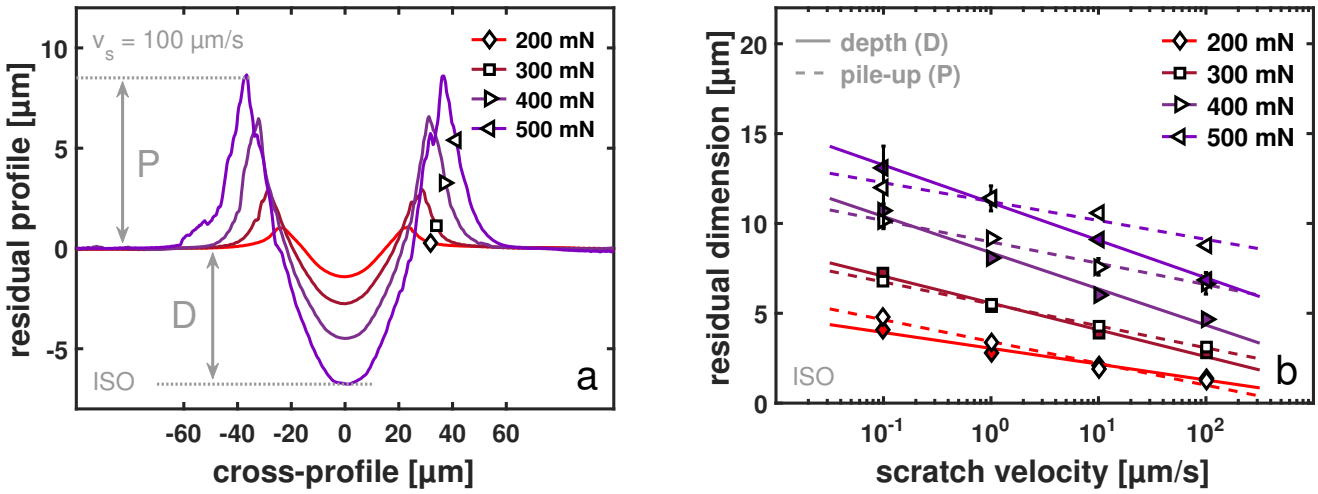

Figure 3: a) Cross-profile averaged over the steady-state scratch section of scratch tests performed at 100 µm/s on isotropic samples. Highest applied normal load shows cracking close to the pile-up maximum on the inner side of the scratch, indicating the position of highest hydrostatic stress. b) Residual depth and pile-up height for different combinations of applied load and scratch velocity. Pile-up height (dominated by large deformations) has a constant rate dependency, while the rate dependence of the depth (governed by the viscoelastic and plastic zone) is a function of the absolute value of surface penetration.

deduced from the data of Caelers et al. [38]).

The residual scratch profile, after the material has recovered, is measured with an optical profilometer. The residual scratch profile depends on the scratch velocity, and the depth and pile-up both increase with decreasing deformation rate. For different applied loads an average cross-profile is taken in the steady-state regime and presented in Figure 3a. The residual depth and pile-up height are indicated with the letter D and P, respectively. The residual dimensions of the depth and the pile-up, presented in Figure 3b, confirm that the pile-up height is increased with increasing normal load, however its rate dependency is not affected. The component of the deformation kinetics that governs the recovery, the material's elasticity, is fundamentally rate independent and hence the absolute recovery (in µm) is expected to be rate independent. The velocity dependence of the residual depth is found to be equal to the velocity dependence of the in-situ penetration.

In glassy polymers, when locally stresses become larger than a critical hydrostatic stress [42–45], material failure is observed. The residual topography of an experiment with $F_n = 500$ mN shows failure of the sample with periodic cracks at both edges of the pile-up, slightly closer to the pile-up maximum on the inner side, a bit further downhill on the outer side of the scratch. From the average cross-profiles (Figure 3a) this local failure can be clearly seen; whereas for $F_n = 200$ mN the residual profile is completely smooth, it gradually turns irregular with increasing load and for $F_n = 500$ mN eventually shows discontinuities, i.e. cracks. Due to tensile forces present behind the indenter tip, these initiated micro-cracks are opened upon continuation of the scratch experiment. An external force is needed to do so, hence the lateral force measured for a load of 500 mN is higher than to be expected for ductile deformation.

Oriented polypropylene

From the oriented polypropylene tapes, test samples are obtained in the two principal directions, parallel and perpendicular to the orientation direction. As a result of the imposed orientation, uniaxial tensile experiments on the extruded tape (DR-1.1) show a different response depending on the orientation of the machined tensile bar. Samples cut along the machine direction have a defined yield point, after which a decrease in tensile stress is observed upon further deformation, see Figure 4a. Normally, in a tensile experiment this would imply localisation and necking, however oriented iPP deforms homogeneously instead of necking. Upon further deformation the stress increases again, and the deformed material enters the strain hardening regime. The tensile curve obtained in machine direction is therefore a reliable approximation of the intrinsic material behaviour. In transverse direction on the other hand, due to the orientation of the entangled network in this direction the sample localizes and necks already before reaching the yield point. Since still significant strain hardening is present, the DR-1.1 TD sample can be stretched over 400% before it fails.

Increasing the draw ratio to DR-2 has an enormous effect on the tensile response. In the direction of crystal orientation the more extended chains do not show a distinct yield point, but significant hardening due to the pre-stretch is already present at lower strains, increasing the tensile stress. The maximum elongation is limited to around 120% (Figure 4b). The orientation of the entangled network however decreases the mechanical performance in transverse direction. Despite a slight increase in yield stress, the material fails already after 55% of elongational

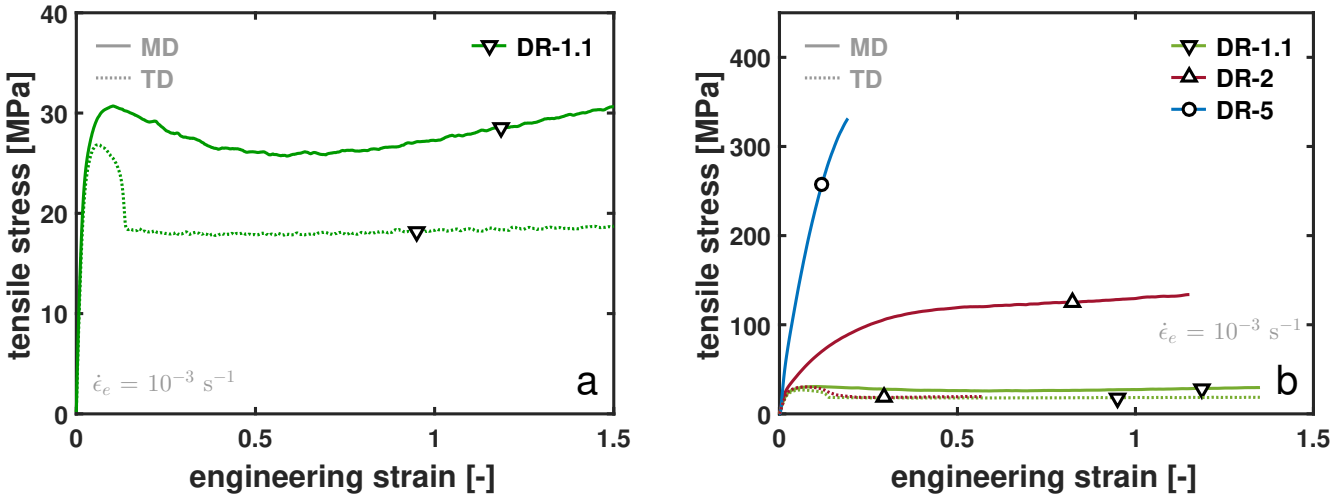

Figure 4: Tensile response of oriented α-iPP samples. a) Machine- and transverse direction for DR-1.1, displaying substantial higher strain hardening in MD than in TD, yet sufficient hardening in TD to allow for large-strain plastic deformation. b) MD and TD for the samples DR-1.1 and DR-2, and MD for sample DR-5, showing an increase in maximum stress upon increasing pre-stretch. TD could not be measured for sample DR-5 due to inhomogeneities reducing the sample dimensions.

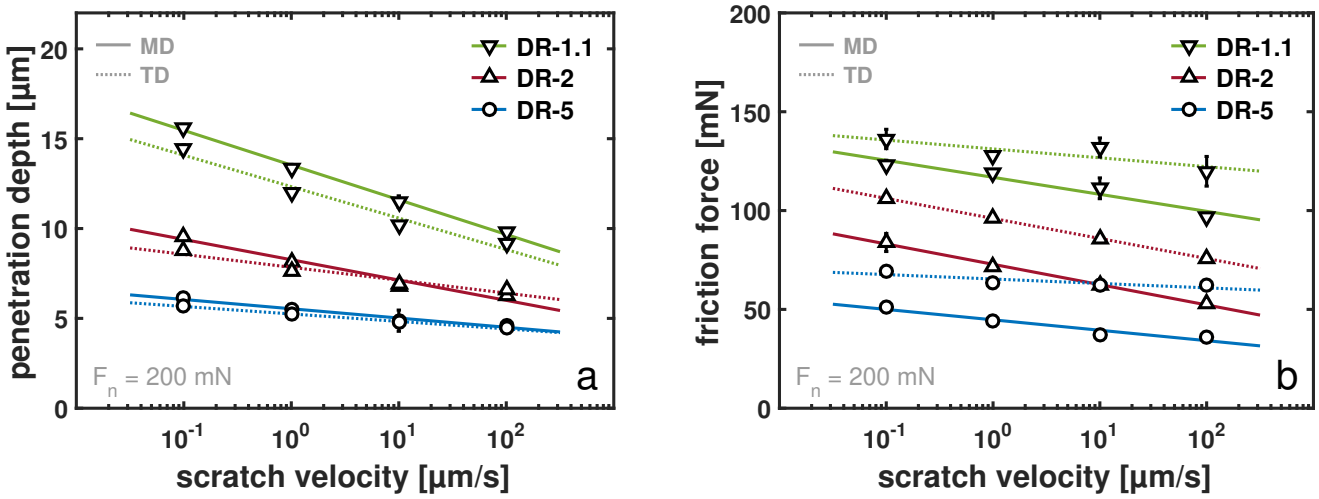

Figure 5: a) Penetration depth as function of sliding velocity for different amounts of orientation. In both machine direction (MD) as transverse direction (TD) a normal load of 200 mN is applied. b) Corresponding lateral force, being substantially higher when sliding in TD as compared to sliding in MD.

strain compared to 400% for the DR-1.1 sample. The sample with a pre-stretch factor of 5, DR-5, possesses a maximum stress over ten times larger than the DR-1.1 sample, yet fails after 20% due the destruction of the highly oriented network. Due to limiting sample dimensions no tensile bars could be machined in perpendicular direction. However, based on the results of DR-2 in transverse direction and the observations of Van Erp [37], no increase in maximum stress is expected. Notwithstanding a combination of extreme localization and less hardening in that direction reduce the strain-at-break even further, possibly to strains lower than the theoretical strain at yield.

In the following, the scratch response for the oriented iPP is related to intrinsic material behaviour, which is not directly measured but qualitatively assessed from the uniaxial tensile experiments presented in the antecedent paragraph. For the various draw ratios the scratch response is measured under a constant load of 200 mN and different sliding velocities. The penetration depth, Figure 5a, decreases with increasing amount of pre-stretch due to the overall increase in network stiffness. Although the yield stress in transverse direction hardly increases, the strongly oriented network in machine direction hinders the penetration. The plastic zone beneath the indenter tip is in isotropic samples dominated by the viscoelastic pre-yield regime, but in highly oriented samples governed by hardening effects that are present already at low strains (Figure 4). It should be taken into account that independent of the sliding direction, the initial indentation step is always in the normal direction (ND), i.e. perpendicular to the orientation direction. The tension caused by pre-stretching the material hinders this transverse deformation, decreasing the initial surface penetration. Subsequent sliding in machine direction implies that the material in front of the tip is pushed sideways, thus into the transverse direction. Due to the low resistance against deformation in TD, this is relatively easy, hence the indenter tip is not lifted much. On the other hand, sliding in TD means that material in front of the tip is at some point pushed towards the MD, the direction of most strain hardening. The large resistance against deformation in MD results in an accumulation of material in front of the indenter tip, slightly lifting the tip.

The directional dependence of the penetration depth is however negligible compared to that of the frictional resistance (Figure 5b). Although the penetration depth is comparable or slightly lower in TD, and on the basis of that a lower friction force would be expected, the accumulation of material in the bow-wave explains the much higher friction force obtained in TD as compared to MD. The residual scratch profiles obtained by optical profilometry (Figure 6) perfectly depicts this significant direction dependence. By looking at the cross-profile (Figure 6a) it can be seen that after sliding in the transverse direction the pile-up is very steep at the outer side of the scratch, indicating a higher resistance in machine direction. The lateral profile (Figure 6b) shows this higher resistance in MD in a different way. In this plot the machine direction is out of the paper-plane for the TD profile. Deformation in that direction is limited, hence we observe a large accumulation of material in front of the tip, much larger than for the MD profile, where the direction of largest resistance is in-plane and thus material accumulation is very little. The increasing de-localization in orientation direction and localization in transverse direction, yields a smooth residual scratch after sliding in MD, while in TD the roughness (characterized by the pile-up frequency in Figure 6b) increases compared to isotropic material. The onset of wear, preceded by a decrease in frequency, is delayed by orienting iPP and subsequent sliding in orientation direction, while

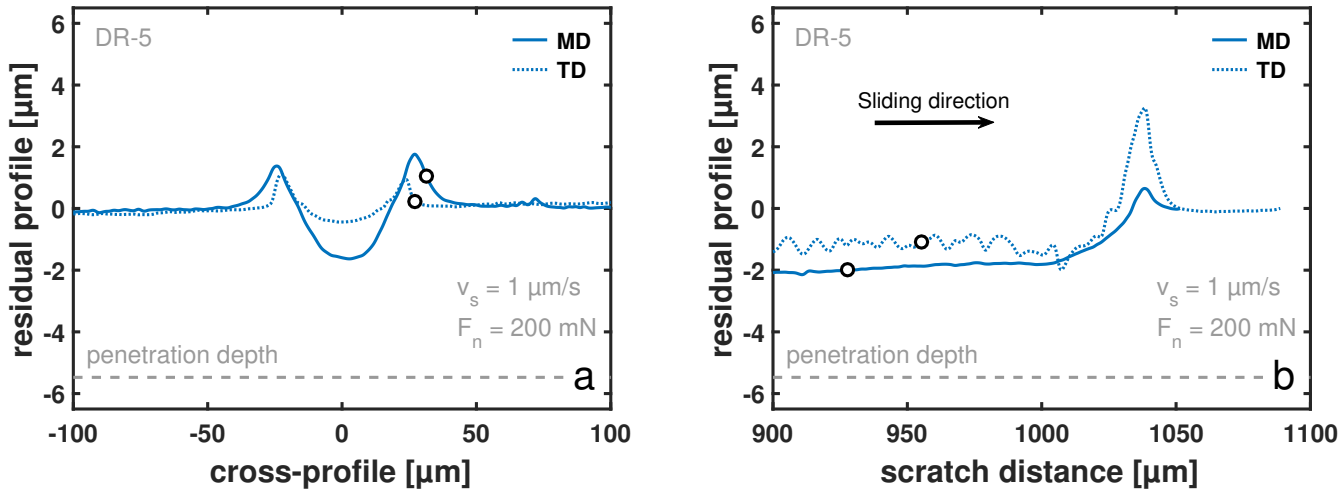

Figure 6: a) Residual cross-profiles for a DR-5 sample subjected to a sliding friction experiment in MD and TD. In-situ penetration depth and test conditions are indicated in the plot. Strain hardening limits the sidewards deformation of the pile-up when sliding in TD. b) Corresponding lateral profile. The limited outward deformation when sliding in TD builds up an enormous bow wave in front of the indenter tip, being the cause of the high frictional resistance observed.

sliding in transverse direction accelerates the accumulation of plastic strain facilitating local fracture. However, the decreasing surface penetration in TD, leads to an overall decrease in plastic strain, delaying crack initiation and subsequently wear. In other words, under a given loading condition, the ductile to brittle transition as defined by Briscoe [9, 11, 12, 46], shifts to higher normal loads.

If the samples DR-1.1 and DR-5 are compared, the decreasing surface penetration with increasing pre-stretch lowers the absolute frictional resistance, whereas the relative difference between MD and TD seems not to be affected, implying a negligible effect of strain hardening. This is explained by the interplay of penetration depth and hardening; lowering the surface penetration automatically means less deformation and therefore less accumulation of material in front of the tip. If the load on the DR-5 sample is increased to 500 mN, the steady-state surface penetration is comparable to that of DR-1.1 at $F_n = 200$ mN, yet the absolute difference in lateral force between MD and TD is increased by about a factor of 10, see Figure 7, confirming the significant effect of orientation.

To study the effect of applied normal load on oriented iPP, the DR-5 sample is selected since the amount of anisotropy is highest. Normal loads ranging from 200 mN to 500 mN are applied on the oriented surface and sliding-friction experiments are performed in MD and TD. Upon

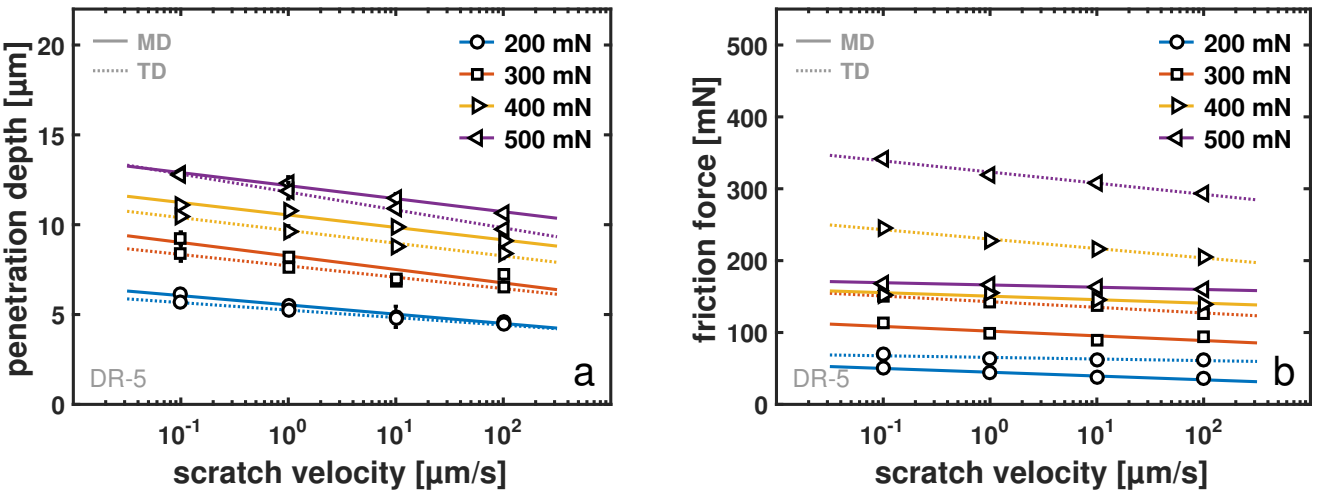

Figure 7: a) Penetration depth as function of applied sliding velocity on sample DR-5 for increasing normal load. b) Corresponding steady-state frictional force measurements. The increasing ratio between TD and MD is rather caused by a down-shift of the force in MD than by an up-shift of the force in TD.

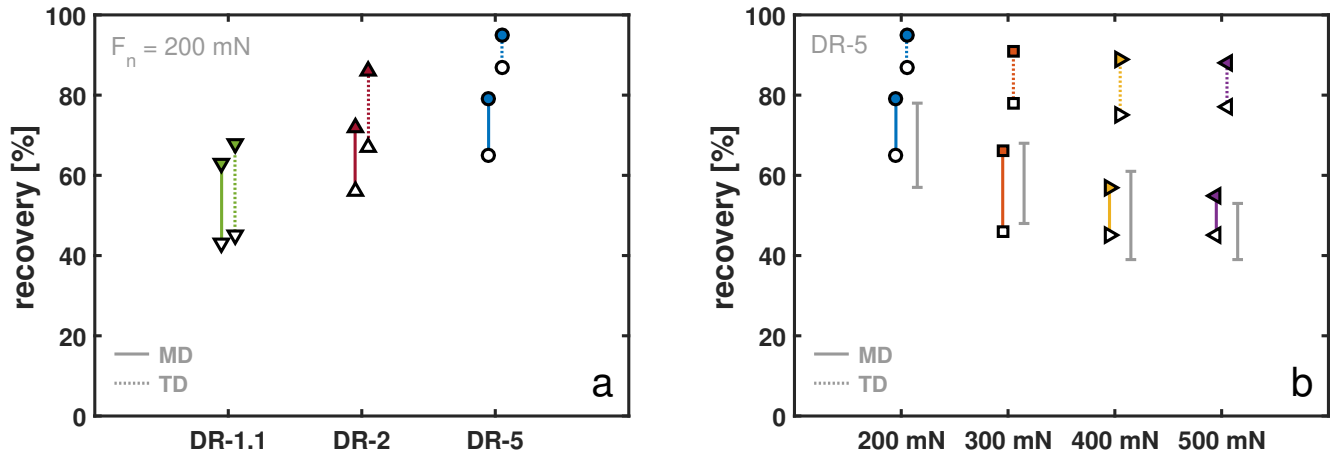

Figure 8: a) Recovery percentage for the different samples tested at 200 mN. The vertical bars indicate the range of recovery percentages found for different applied sliding velocities; the open symbols correspond to a sliding velocity of 0.1 µm/s, whereas the filled symbols indicate a velocity of 100 µm/s. b) Elastic recovery percentages for MD and TD as function of applied load. Results of the isotropic α-phase are shown by vertical (gray) bars without a marker.

increasing load the surface penetration increases with equal amount in both directions (Figure 7a). The effect however is less pronounced compared to the isotropic α-phase iPP shown in Figure 2a. This can be attributed to the repulsive tensile forces in the oriented semi-crystalline "strings" that develop upon (transverse) indentation. The proof for this hypothesis can already be seen from the lateral force plot in Figure 7b; whereas the frictional force in TD shifts linearly with applied normal load, in MD this shift upward decreases with increasing load. This implies that indeed the difference in hardening is causing the larger directional incongruence in lateral force. The induced tensile stress in the material facilitates sliding in the machine direction and pulls the material in front of the tip underneath it, therewith reducing the accumulation of strain in front of the indenter head.

The final material property that should be discussed is the remarkable elastic recovery of the solid-state drawn samples. Despite the large bow-wave and high lateral force encountered when sliding in the TD, the elastic recovery can go up to 95% for samples with a stretch ratio of 5, see Figure 8a. Oriented crystals and the connecting amorphous network in MD experience high tensile forces over a relatively large area when deformed in transverse direction. The combined retraction force of this large area acts as a "string", leading to a remarkably high elasticity. The increase of elasticity in TD is more pronounced than in MD, due the combined effect of increasing orientation and decreasing surface penetration. The recovery in MD on the other hand, is promoted by the decrease in penetration depth with increasing orientation, but decreased again by the loss of network stiffness in transverse direction. Comparing the recovery of the sample DR-5 for the various applied normal loads (Figure 8b), as expected in both principal directions it decreases with increasing load, due to the larger overall deformations. Compared to isotropic samples (gray bars) the recovery in MD is not much affected, while in TD the elastic recovery is substantially increased.

4. Conclusions

Comparable to previous studies on glassy polymers and epoxies, the steady-state penetration into the surface of isotropic isotactic polypropylene is found to be governed by the pre-yield viscoelastic response. A lower sliding velocity yields time for relaxation, and hence the penetration into the surface is deeper. Applying a higher normal load intuitively results in a deeper penetration, because when a higher force is applied on the same contact area, the stresses and respectively the strains are higher. As long as the deformation is ductile, the lateral force increases according to the penetration depth. Upon local brittle failure, the measured frictional resistance increases. Due to the negligible viscous effects in the large-strain regime of iPP, the friction force is found to have a constant rate dependency.

Orientation of the alternating crystal- and amorphous layers makes the material in machine direction remarkably more scratch resistant. Surface penetration perpendicular to the orientation direction is hindered by in-plane tension resulting in a direction independent in-situ scratch depth that decreases upon increasing the amount of pre-stretch. In machine direction, the anisotropic crystal structure facilitates lateral deformation of the bow-wave reducing the friction force. In addition, the tension in the stretched network pulls part of the material underneath the indenter tip, reducing the lateral force even further. The orientation of the semi-crystalline network obstructs sideways

deformation of the bow-wave when sliding in transverse direction, accumulating material in front of tip. The therewith increased frictional resistance in TD, compared to MD, leads to an increase in energy dissipation and the scratch resistance reduces. Under the same loading conditions however, isotropic iPP shows, due to the lack of the transverse network stiffness, a much higher surface penetration. In this respect, local- and global strains are decreased and therewith the onset of wear in both principal directions can be delayed by solid-state orientation. The residual scratch depth is substantially reduced compared to isotropic samples as well, due to the retraction of the highly oriented strings. In general the scratch resistance in isotactic polypropylene can thus be significantly enhanced by orientation.

Acknowledgements

The authors wish to thank Royal DSM N.V. for their valuable assistance in sample orientation, and Giuseppe Portale for providing us with X-ray beam-time for sample characterization.

Additional Information

The authors declare no competing interests.

References

[1] J. Fu, B. W. Ghali, A. J. Lozynsky, E. Oral, O. K. Muratoglu, Wear resistant UHMWPE with high toughness by high temperature melting and subsequent radiation cross-linking, Polymer 52 (4) (2011) 1155–1162. doi:10.1016/j.polymer.2011.01.017.

[2] O. K. Muratoglu, C. R. Bragdon, D. O. O'Connor, M. Jasty, W. H. Harris, G. Rizwan, F. McGarry, Unified wear model for highly crosslinked ultra-high molecular weight polyethylenes (UHMWPE), Biomaterials 20 (16) (1999) 1463–1470. doi:10.1016/S0142-9612(99)00039-3.

[3] A. A. Edidin, L. Pruitt, C. W. Jewett, D. J. Crane, D. Roberts, S. M. Kurtz, Plasticity-induced damage layer is a precursor to wear in radiation- cross-linked UHMWPE acetabular components for total hip replacement, Journal of Arthroplasty 14 (5) (1999) 616–627. doi:10.1016/S0883-5403(99)90086-4.

[4] S. A. Atwood, D. W. Van Citters, E. W. Patten, J. Furmanski, M. D. Ries, L. A. Pruitt, Tradeoffs amongst fatigue, wear, and oxidation resistance of cross-linked ultra-high molecular weight polyethylene, Journal of the Mechanical Behavior of Biomedical Materials 4 (7) (2011) 1033–1045. doi:10.1016/j.jmbbm.2011.03.012.

[5] E. Oral, K. K. Wannomae, N. Hawkins, W. H. Harris, O. K. Muratoglu, α-Tocopherol-doped irradiated UHMWPE for high fatigue resistance and low wear, Biomaterials 25 (24) (2004) 5515–5522. doi:10.1016/j.biomaterials.2003.12.048.

[6] F. Renò, M. Cannas, UHMWPE and vitamin E bioactivity: An emerging perspective (2006). doi:10.1016/j.biomaterials.2006.01.016.

[7] B. J. Briscoe, P. D. Evans, S. K. Biswas, S. K. Sinha, The hardnesses of poly(methylmethacrylate), Tribology International 29 (2) (1996) 93–104. doi:10.1016/0301-679X(95)00045-6.

[8] B. J. Briscoe, E. Pelillo, S. K. Sinha, Scratch hardness and deformation maps for polycarbonate and polyethylene, Polymer Engineering and Science 36 (24) (1996) 2996–3005. doi:Doi10.1002/Pen.10702.

[9] B. J. Briscoe, S. K. Sinha, Wear of polymers, Proceedings of the Institution of Mechanical Engineers, Part J: Journal of Engineering Tribology 216 (6) (2002) 401–413. doi:10.1243/135065002762355325.

[10] W. Brostow, H. E. Hagg Lobland, M. Narkis, Sliding wear, viscoelasticity, and brittleness of polymers, Journal of Materials Research 21 (09) (2006) 2422–2428. doi:10.1557/jmr.2006.0300.

[11] B. J. Briscoe, Isolated contact stress deformations of polymers: The basis for interpreting polymer tribology, in: Tribology International, Vol. 31, 1998, pp. 121–126. doi:10.1016/S0301-679X(98)00014-0.

[12] B. J. Briscoe, S. K. Sinha, Scratch Resistance and Localised Damage Characteristics of Polymer Surfaces - A Review, Materwis Werkstofftech 34 (10-11) (2003) 989–1002. doi:10.1002/mawe.200300687.

[13] Y. J. Mergler, R. J. Van Kampen, W. J. Nauta, R. P. Schaake, B. Raas, J. G. Van Griensven, C. J. Meesters, Influence of yield strength and toughness on friction and wear of polycarbonate, Wear 258 (5-6) (2005) 915–923. doi:10.1016/j.wear.2004.09.046.

[14] W. Brostow, W. Chonkaew, R. Mirshams, A. Srivastava, Characterization of grooves in scratch resistance testing, in: Polymer Engineering and Science, Vol. 48, 2008, pp. 2060–2065. doi:10.1002/pen.21085.

[15] V. Jardret, H. Zahouani, J. Loubet, T. Mathia, Understanding and quantification of elastic and plastic deformation during a scratch test, Wear 218 (1) (1998) 8–14. doi:10.1016/S0043-1648(98)00200-2.

[16] C. Gauthier, R. Schirrer, Time and temperature dependence of the scratch properties of poly(methylmethacrylate) surfaces, Journal of Materials Science 35 (9) (2000) 2121–2130. doi:10.1023/A:1004798019914.

[17] I. Demirci, C. Gauthier, R. Schirrer, Mechanical analysis of the damage of a thin polymeric coating during scratching: Role of the ratio of the coating thickness to the roughness of a scratching tip, Thin Solid Films 479 (1-2) (2005) 207–215. doi:10.1016/j.tsf.2004.11.194.

[18] J. H. Lee, G. H. Xu, H. Liang, Experimental and numerical analysis of friction and wear behavior of polycarbonate, Wear 251 (PART 2) (2001) 1541–1556. doi:Doi:10.1016/s0043-1648(01)00788-8.

[19] J. L. Bucaille, C. Gauthier, E. Felder, R. Schirrer, The influence of strain hardening of polymers on the piling-up phenomenon in scratch tests: Experiments and numerical modelling, Wear 260 (7-8) (2006) 803–814. doi:10.1016/j.wear.2005.04.007.

[20] H. Jiang, G. T. Lim, J. N. Reddy, J. D. Whitcomb, H. J. Sue, Finite element method parametric study on scratch behavior of polymers, in: Journal of Polymer Science, Part B: Polymer Physics, Vol. 45, 2007, pp. 1435–1447. arXiv:0406218, doi:10.1002/polb.21169.

[21] N. Aleksy, G. Kermouche, A. Vautrin, J. M. Bergheau, Numerical study of scratch velocity effect on recovery of viscoelastic-viscoplastic solids, International Journal of Mechanical Sciences 52 (3) (2010) 455–463. doi:10.1016/j.ijmecsci.2009.11.006.

[22] H. Pelletier, C. Gauthier, R. Schirrer, Influence of the friction coefficient on the contact geometry during scratch onto amorphous polymers, Wear 268 (9-10) (2010) 1157–1169. doi:10.1016/j.wear.2010.01.003.

[23] Z. Wang, P. Gu, H. Zhang, Z. Zhang, X. Wu, Finite element modeling of the indentation and scratch response of epoxy/silica nanocomposites, Mechanics of Advanced Materials and Structures 21 (10). doi:10.1080/15376494.2012.707752.

[24] M. M. Hossain, R. Minkwitz, P. Charoensirisomboon, H. J. Sue, Quantitative modeling of scratch-induced deformation in amorphous polymers, Polymer (United Kingdom) 55 (23) (2014) 6152–6166. doi:10.1016/j.polymer.2014.09.045.

[25] B. Feng, Z. Chen, Tribology behavior during indentation and scratch of thin films on substrates: Effects of plastic friction, AIP Advances 5 (5). doi:10.1063/1.4921836.

[26] L. C. A. Van Breemen, L. E. Govaert, H. E. H. Meijer, Scratching polycarbonate: A quantitative model, Wear 274-275 (2012) 238–247. doi:10.1016/j.wear.2011.09.002.

[27] S. Krop, H. E. Meijer, L. C. Van Breemen, Finite element modeling and experimental validation of single-asperity sliding friction of diamond against reinforced and non-filled polycarbonate, Wear 356-357 (2016) 77–85. doi:10.1016/j.wear.2016.03.014.

[28] T. Tervoort, R. Smit, W. Brekelmans, L. Govaert, A Constitutive Equation for the Elasto-Viscoplastic Deformation of Glassy Polymers, Mechanics Time-Dependent Materials 1 (3) (1997) 269–291. doi:10.1023/A:1009720708029.

[29] E. T. Klompen, T. A. Engels, L. E. Govaert, H. E. Meijer, Modeling of the postyield response of glassy polymers: Influence of thermomechanical history, Macromolecules 38 (16) (2005) 6997–7008. doi:10.1021/ma050498v.

[30] L. C. A. Van Breemen, E. T. J. Klompen, L. E. Govaert, H. E. H. Meijer, Extending the EGP constitutive model for polymer glasses to multiple relaxation times, Journal of the Mechanics and Physics of Solids 59 (10) (2011) 2191–2207. doi:10.1016/j.jmps.2011.05.001.

[31] D. J. Senden, S. Krop, J. A. Van Dommelen, L. E. Govaert, Rate- and temperature-dependent strain hardening of polycarbonate, Journal of Polymer Science, Part B: Polymer Physics 50 (24) (2012) 1680–1693. doi:10.1002/polb.23165.

[32] L. C. Van Breemen, T. A. Engels, E. T. Klompen, D. J. Senden, L. E. Govaert, Rate- and temperature-dependent strain softening in solid polymers, Journal of Polymer Science, Part B: Polymer Physics 50 (24) (2012) 1757–1771. doi:10.1002/polb.23199.

[33] S. Krop, H. E. Meijer, L. C. Van Breemen, Global and local large-deformation response of sub-micron, soft- and hard-particle filled polycarbonate, Journal of the Mechanics and Physics of Solids 87 (2016) 51–64. doi:10.1016/j.jmps.2015.11.005.

[34] S. Krop, H. E. Meijer, L. C. Van Breemen, Multi-mode modeling of global and local deformation, and failure, in particle filled epoxy systems, Composites Part A: Applied Science and Manufacturing 88 (2016) 1–9. doi:10.1016/j.compositesa.2016.05.012.

[35] J. W. Housmans, M. Gahleitner, G. W. M. Peters, H. E. H. Meijer, Structure-property relations in molded, nucleated isotactic polypropylene, Polymer 50 (10) (2009) 2304–2319. doi:10.1016/j.polymer.2009.02.050.

[36] M. van Drongelen, T. van Erp, G. Peters, Quantification of non -isothermal, multi-phase crystallization of isotactic polypropylene :The influence of cooling rate and pressure, Polymer 53 (21) (2012) 1–12. doi:10.1016/j.polymer.2012.08.003.

[37] T. B. Van Erp, C. T. Reynolds, T. Peijs, J. A. W. Van Dommelen, L. E. Govaert, Prediction of yield and long-term failure of oriented polypropylene: Kinetics and anisotropy, Journal of Polymer Science, Part B: Polymer Physics 47 (20) (2009) 2026–2035. arXiv:0406218, doi:10.1002/polb.21801.

[38] H. J. Caelers, E. Parodi, D. Cavallo, G. W. Peters, L. E. Govaert, Deformation and failure kinetics of iPP polymorphs, Journal of Polymer Science, Part B: Polymer Physics 55 (9) (2017) 729–747. doi:10.1002/polb.24325.

[39] W. Bras, I. P. Dolbnya, D. Detollenaere, R. Van Tol, M. Malfois, G. N. Greaves, A. J. Ryan, E. Heeley, Recent experiments on a combined small-angle/wide-angle X-ray scattering beam line at the ESRF, in: Journal of Applied Crystallography, Vol. 36, 2003, pp. 791–794. doi:10.1107/S002188980300400X.

[40] B. Lotz, S. Graff, J. C. Wittmann, Crystal morphology of the γ (triclinic) phase of isotactic polypropylene and its relation to the α phase, Journal of Polymer Science Part B: Polymer Physics 24 (9) (1986) 2017–2032. doi:10.1002/polb.1986.090240909.

[41] A. T. Jones, J. M. Aizlewood, D. R. Beckett, Crystalline forms of isotactic polypropylene, Die Makromolekulare Chemie 75 (1) (1964) 134. doi:10.1002/macp.1964.020750113.

[42] M. Ishikawa, I. Narisawa, H. Ogawa, Criterion for craze nucleation in polycarbonate, Journal of Polymer Science: Polymer Physics Edition 15 (10) (1977) 1791–1804. doi:10.1002/pol.1977.180151009.

[43] R. P. Kambour, E. A. Farraye, Crazing beneath notches in ductile glassy polymers: a materials correlation., Polym. Commun. 25 (12) (1984) 357–360.

[44] R. P. Nimmer, J. T. Woods, An investigation of brittle failure in ductile, notchsensitive thermoplastics, Polymer Engineering & Science 32 (16) (1992) 1126–1137. doi:10.1002/pen.760321610.

[45] T. A. Engels, L. C. Van Breemen, L. E. Govaert, H. E. Meijer, Criteria to predict the embrittlement of polycarbonate, Polymer 52 (8) (2011) 1811–1819. doi:10.1016/j.polymer.2011.02.027.

[46] B. Briscoe, Wear of polymers: an essay on fundamental aspects, Tribology International 14 (4) (1981) 231–243. doi:10.1016/0301-679X(81)90050-5.